FOREX Publication
Open Access | Rapid and quality publishing

International Journal of
Electrical and Electronics Research (IJEER)
Research Article | Volume 9, Issue 4 | Pages 107-113 | e-ISSN: 2347-470X

REULEAUX Triangle Shaped MSPA for 5G and WLAN Applications

Mahesh Shankar Pandey [1] and Dr. Virendra Singh Chaudhary[2]

[1]*Research Scholar, DoECE, RKDF University, India*
[2]*Professor, DoECE, RKDF University, Bhopal, M.P., India*

***Correspondence:** Mr. Mahesh Shankar Pandey; Email: mshankarpandey21@gmail.com

ABSTRACT: This research work proposes a low-key REULEAUX Triangle Shaped antenna having a square, rectangular Patch attached through the feedline. This antenna has REULEAUX Triangle as a patch element with a bottom having square-shaped geometry to attain ultra-wideband characteristics. This compact wideband antenna for WLAN, 5G and WiMAX applications has been presented in this manuscript. The compact antenna (60×65×1.6 mm^3) is intended and manufactured on a substrate of FR-4 material and evaluated on different grounds to validate the performance. The comparison of simulated results and measured outcomes reveal that the proposed device has return loss ($|S_{11}|$) < -10 dB along with 4.272 GHz impedance BW between 1.738 GHz and 6.01 GHz covering ultra-wideband region. In the measured outcomes, it is clear that the proposed REULEAUX Triangle Shaped antenna has radiation with omnidirectional characteristics with the peak gain of 2.75dB in the operating band. The antenna also attains 110.26% fractional bandwidth in the operating band. Cost of construction of antenna is very low due to easy availability and budget price of the material used. These outcomes with large bandwidth and steady radiation patterns prove that the proposed antenna design will be appropriate for UWB applications.

Keywords: Microstrip Antenna, 5G, WLAN, REULEAUX Triangle, ultra-wideband

ARTICLE INFORMATION

Author(s): Mahesh Shankar Pandey, Dr. Virendra Singh Chaudhary
Received: Sep 12, 2021; **Accepted**: Dec 11, 2021; **Published**: Dec 30, 2021;
e-ISSN: 2347-470X;
Paper Id: IJEER120108;
Citation: doi.org/10.37391/IJEER.090403
Webpage-link:
https://ijeer.forexjournal.co.in/archive/volume-9/ijeer-090403.html

1. INTRODUCTION

Nowadays, ultra-wideband (UWB) wireless communication has a huge demand because of its endless striking features. For example, less power-hungry, rapid operation, lower disturbances, and higher quality of service. Additionally, this innovation acquired expanded prominence when UWB is agreed on access to viable applications, particularly 5G, WiMAX, and WLAN [1]. Because the antenna is a primary part of the communication system and that decides the performance as far as capacity, data rate, and efficiency are concerned. A device with great transmission attributes, enormous bandwidth and less cross-polarization has turned into an exploration area of interest in the various domains, e.g. modern portable devices, sensing radars, and remote surveillance [2, 3]. Whether [3] has multiple bands of operation that can limit the antenna usability to specific applications like WiMAX or WLAN. Quite a lot of antennas have been planned and employed for such wideband applications, like Vivaldi [4], horn [5], planer [6], and log periodic shaped antennas [7]. Among these shapes, the Vivaldi antenna has exhibited a wider operational band. The horn shapes are suitable for long-range applications and cannot fulfil domestic or consumer applications, which UWB antennas can achieve. In a few experiments [9], changing the wide slot's position, including shifting the rotation, will also be helpful to get the broader band of the antenna. The side of the wide slot can also create an impact to change the position in center frequency along with the shifting of lower cutoff and higher cutoff frequencies [10]. However, High Gain with a broader bandwidth antenna with utmost radiation attributes has been acknowledged late. The operational bandwidth of the antenna can be enhanced by implementing the metamaterial in the fabrication of the antenna [11]. The use of metamaterial also increases the directivity. In [11], even after using metamaterial, the antenna bandwidth is not comprehensive, covering multiple operational bands.

After a deep analysis of the following research work, these a large scope to get such an antenna geometry with broader bandwidth and capable of covering larger consumer applications mentioned here. The advantages of such geometry will reduce the burden of multiple hardware for different wireless technologies, and even in future, such designs can be miniaturized to fit into Nano devices.

Reported antenna found itself a good candidate for broadband wireless services such as personal communication services (1.85-1.99 GHz), WiMAX (2.5 GHz, 3.5 GHz and 5.5 GHz) and WLAN (2.4 GHz, 5.2 GHz and 5.8 GHz). The performance characteristics such as antenna design, parametric analysis, input impedance, simulated surface current distribution, simulated and measured return loss, radiation pattern and gain of reported antenna have been analyzed.

FOREX Publication
Open Access | Rapid and quality publishing
International Journal of Electrical and Electronics Research (IJEER)
Research Article | Volume 9, Issue 4 | Pages 107-113 | e-ISSN: 2347-470X

2. MATERIAL AND METHODS

2.1 Antenna Design

Proposed antenna design results from various design experiments and the corrections made to get the optimal results of the desired operating frequency bands. These experiments are starts from the very basic rough architecture, either circular shape or rectangular shape. After making significant changes in these shapes to get unique geometry, they will be going through the simulation phase, and the various results have been observed to check its suitability for the operation. The simulation of the design has been performed in an electromagnetic simulation environment. There are several simulation software available, e.g., CST-MWS, HFSS, IE3D and ADS etc. Our foremost aim while designing the geometry of the antenna is to longer the way of the current. It is clear from the current theory is that the current flows through the surface of the conductor. To make large current flows, one needs to make its path longer in the available surface area. So, the final design should have a geometry with a longer current path in the available surface area.

The longer path results in the wideband or multiple bands wireless applications of the antenna. The evolution of the antenna design has been shown in *Figures 1(a) to 1(d)*.

Figure 1 refers to the four designs of the antenna. 1(a) shows the antenna having a patch, which combines three shapes: 1. REULEAUX Triangle, 2. Square, and 3 Rectangle.

First, REULEAUX Triangle is the resultant of the multiple modifications in the triangular design by making its edges curved at some angle. This design can be made with the intersection area of three circles and a rectangle.

Second, the square shape is the mid path between the feedline and the REULEAUX Triangle. This helps to spread the current coming from the feedline to the patch triangle.

Third, rectangle shape works as a feed line, get power from the port and matches the impedance to minimize the return loss. Its dimension is also finalized after a few design experiments and after profound observation of the S_{11} parameter.

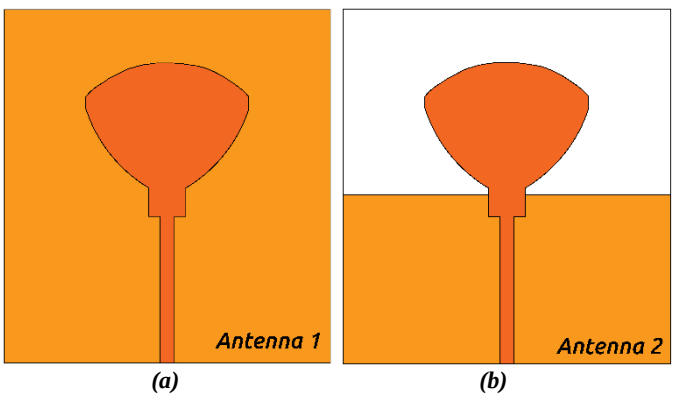

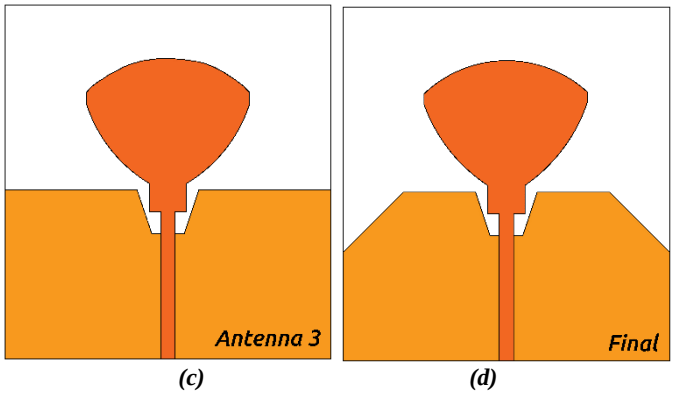

Figure 1: Antenna Design Evolution (a) Antenna 1, (b) Antenna 2, (c) Antenna 3 and (d) Final (Antenna 4)

Above three shapes are the basic building blocks of the antenna patch design. The ground design is rectangle in shape spread across the antenna back surface. And gradually changed as per design evolution. So here are the following designs:

2.1.1 Antenna 1

This antenna geometry contains the patch element combination of the three shapes mentioned above in detail. The Ground is a rectangle in shape without any slot or defection. Between Patch and Ground, there is a substrate of FR4 material having 1.6 mm thickness. The reflection coefficient of this antenna is shown in *Figure 4* curve (i).

2.1.2 Antenna 2

This design has resulted in cutting the ground plane of the structure of Antenna 1. The Ground was cut up-to-the location of a joint of a triangle and square shape. Cutting ground plane reduces the reflection coefficient (S_{11}) < -10 dB between 2 GHz and 3 GHz, and the creation of band see Figure 4 curve (ii).

2.1.3 Antenna 3

The ground plane is further changed by making a notch near the square shape (Patch) in the design of Antenna 2. Making of a notch near feedline location results in the reduction in the return loss (S_{11}) below -10 dB, and creation of two-band one is between 2 GHz and 3 GHz having center frequency near 2.3 GHz, and band 2 is between 3.1 GHz and 5.4 GHz having center frequency 4.35 GHz see Figure 4 curve (iii).

2.1.4 Antenna 4 (Final Geometry)

In the design of Antenna 3, return loss has been achieved with two bands. Extend the antenna's bandwidth and make it suitable for wideband operations. A triangular cut has been made at the top left and right corners of the Ground. These cuts result in the making of a wideband in the return loss ($|S_{11}|$) characteristics below -10 dB, between 1.738 and 6.01 GHz refer to *figure 4* curve (iv).

FOREX Publication
Open Access | Rapid and quality publishing
International Journal of Electrical and Electronics Research (IJEER)
Research Article | Volume 9, Issue 4 | Pages 107-113 | e-ISSN: 2347-470X

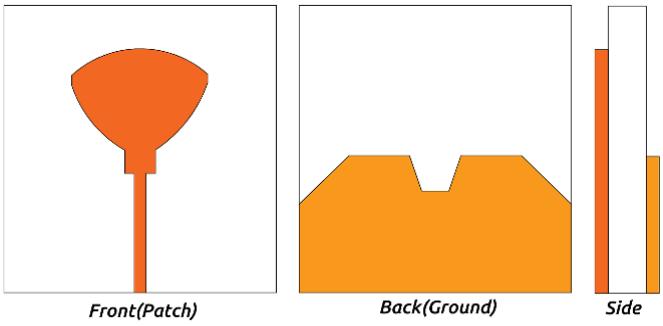

Figure 2: Antenna Structure front view (Patch), back view (Ground) and side view

2.2 Antenna Dimensions

The final geometry of the antenna is shown in *figure 2*. The antenna front view consists Patch of the antenna, and the back view consists Ground of the antenna and the side view. The optimized dimensions are shown the *table 1*. The dimension labels of different parts of the antenna have been shown in *figure 3*. All the dimensions are in mm.

Table 1: Optimized Dimensions of the Antenna (refer Figure 3)

Parameter	Dimension	Parameter	Dimension
W	60 mm	L	65 mm
W_1	13.33 mm	L_1	20 mm
W_2	2.10 mm	L_2	45 mm
W_3	6 mm	L_3	2.08 mm
W_4	2.6 mm	L_4	22.94 mm
W_5	28.68 mm	L_5	1.7 mm
W_6	6.78 mm	L_6	27 mm
G	9.8 mm	S_1	15.56 mm
A_1	33.08 mm	S_2	13.33 mm
A_2, A_3	19.31 mm	h	1.6 mm

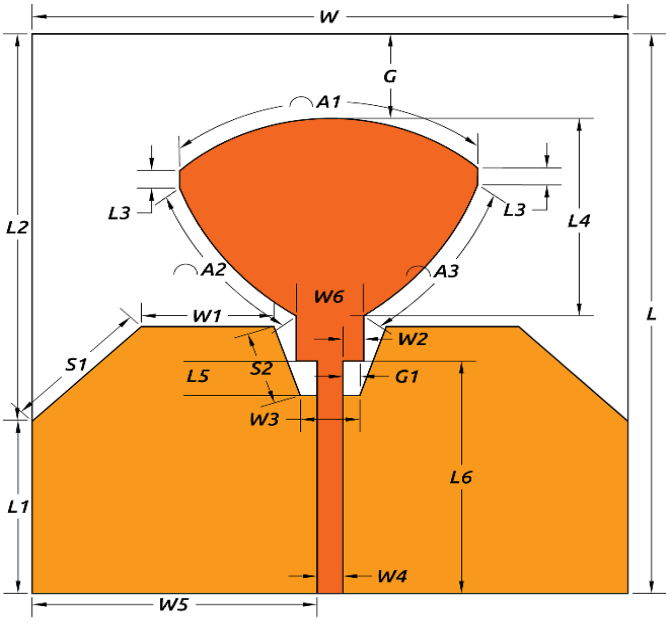

Figure 3: Final Proposed Antenna Design Parameters

3. RESULT AND DISCUSSION

3.1 Return Loss

The simulated return of different versions during antenna evolution has been shown in *figure 4*. The evolution of the antenna is clearly reflected in the return loss characteristics of the antenna. The simulation of antennas was performed from 1 to 7 GHz. The return loss characteristics of the optimised antenna reflect the Bandwidth of 4.272 GHz.

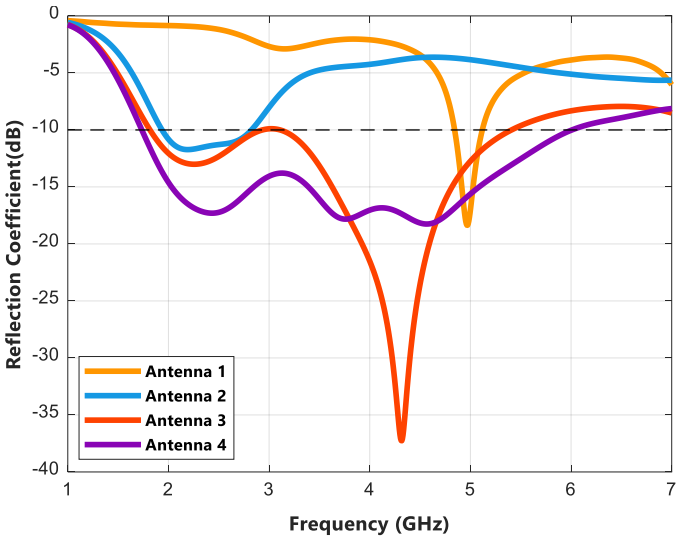

Figure 4: Return loss (S_{11}) characteristics comparison of all antenna designs during evolution

The antenna has been tested in the laboratory to observe the measured results also. The correlation of the simulated and measured return loss has been displayed in Figure 5. The measured results are a bit higher return loss for some frequencies due to manufacturing defects, and environmental losses came through existing microwave radiation of mobile towers, Wi-Fi and other communications setups. For the measurement Anritsu MS2719B Spectrum Analyzer has been used in the anechoic chamber.

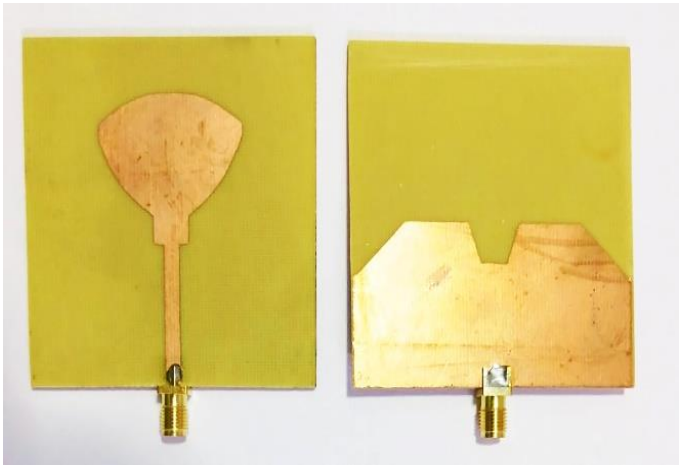

(a)

FOREX Publication
Open Access | Rapid and quality publishing
International Journal of Electrical and Electronics Research (IJEER)
Research Article | Volume 9, Issue 4 | Pages 107-113 | e-ISSN: 2347-470X

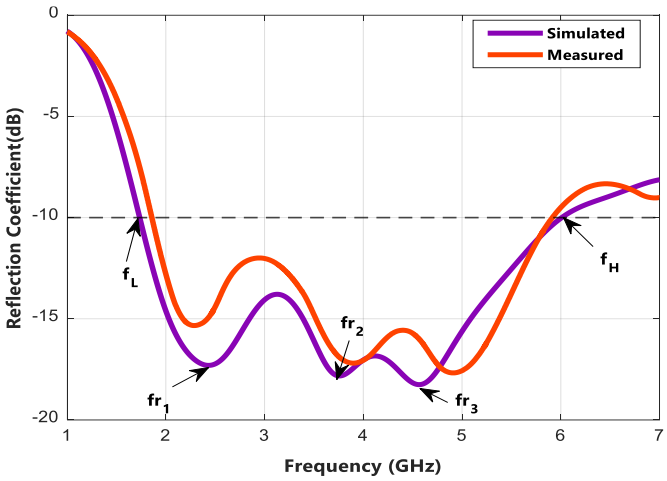

(b)

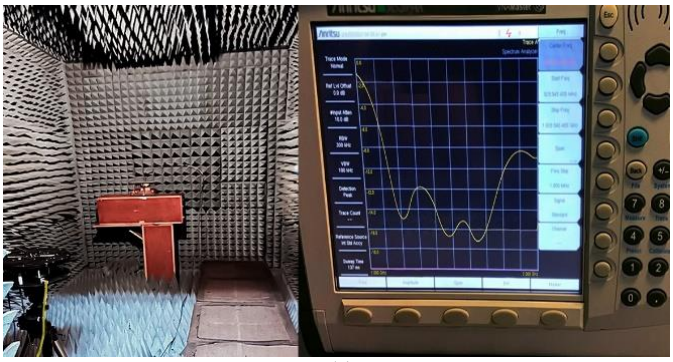

(c)

Figure 5: (a) Fabricated Antenna (b) Simulated vs Measured Return Loss of antenna, (c) Measurement Setup + VNA

Table 2: Different frequencies from simulated and measured outcomes

Frequencies	Simulated	Measured
fr_1	2.434 GHz	2.278 GHz
fr_2	3.760 GHz	3.913 GHz
fr_3	4.564 GHz	4.914 GHz
f_l	1.738 GHz	1.859 GHz
f_h	6.01 GHz	5.915 GHz

3.2 Fractional Bandwidth of Simulated Return Loss

The designed antenna has provided the fractional bandwidth of 110.269% from 1.7381 to 6.01 GHz frequency band for simulated results using Equation (1).

$$\text{Antenna Fractional bandwidth} = 2 \times \left(\frac{f_H - F_L}{f_H + F_L}\right) \% \quad (1)$$

$$= 200 \times \left(\frac{6.01 - 1.7381}{6.01 + 1.7381}\right) \%$$

$$= 200 \times \left(\frac{4.2719}{7.7481}\right) \%$$

$$\text{Antenna Bandwidth} = 110.269\ \%$$

The measured band is between 1.859 GHz to 5.915 GHz having a Bandwidth of 4.056 GHz. The measured results resonate on the 2.278 GHz, 3.913 GHz and 4.914 GHz. The differences are not much and near to simulated outcomes. All frequencies, *e.g.*, lower cutoff, higher cutoff, and resonating frequencies for simulated and measured results, are shown in *table 2*.

3.3 Fractional Bandwidth of Measured Return Loss

The designed antenna has provided the fractional bandwidth of 114.998% from 1.859 to 5.915 GHz frequency band for measured results using *equation (1)*.

$$\text{Antenna Fractional bandwidth} = 200 \times \left(\frac{5.915 - 1.859}{5.915 + 1.859}\right) \%$$

$$= 200 \times \left(\frac{4.056}{7.054}\right) \%$$

$$\text{Antenna Bandwidth} = 114.998\ \%$$

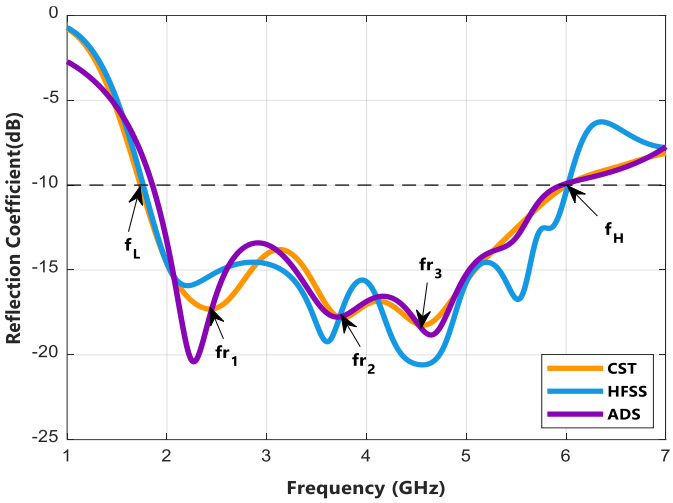

Figure 6: Antenna Return Loss CST vs HFSS vs ADS

3.4 Equivalent Circuit

Figure 7 depicts the equivalent RLC model of the given antenna. It shows the connection of series inductors and parallel capacitors along with resistors. The resultant circuit model was achieved after combining various resonating modes. All resonating frequencies are generated due to different values of L, C and R. The number of L, C or R depends on the return loss matching got from the antenna simulation.

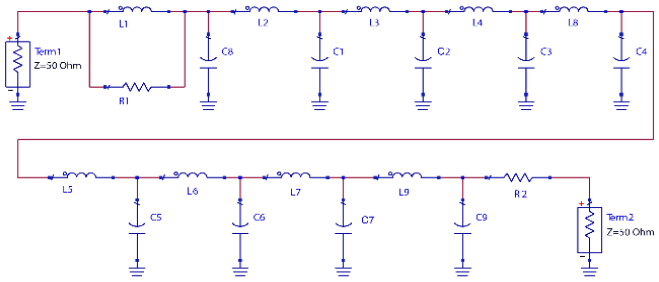

Figure 7: ADS RLC Values

FOREX Publication
Open Access | Rapid and quality publishing
International Journal of Electrical and Electronics Research (IJEER)
Research Article | Volume 9, Issue 4 | Pages 107-113 | e-ISSN: 2347-470X

Table 3: Equivalent RLC Circuit Values from ADS

Components	Values	Components	Values
C_1	0.8237 pF	L_1	1.3960 nH
C_2	0.5837 pF	L_2	16.4528 nH
C_3	0.2696 pF	L_3	1.0544 nH
C_4	0.4511 pF	L_4	0.6649 nH
C_5	0.3672 pF	L_5	0.8764 nH
C_6	0.4016 pF	L_6	5.8519 nH
C_7	0.1952 pF	L_7	10.2757 nH
C	0.1050 pF	L_8	1.99101 nH
C_9	0.0806 pF	R_2	510.18 Ohms
R_1	58.00 Ohms		

Table 4: RLC Values from CST

Components	Values	Components	Values
R_1	0.765 ohms	L_1	0.0035 nH
R_2	1.293 ohms	L_2	0.0012 nH
R_3	1.293 ohms	L_3	0.0012 nH
R_4	1.030 ohms	L_4	0.0105 nH
R_5	1.688 ohms	L_5	0.0496 nH
R_6	1.085 ohms	L_6	0.0218 nH
R_7	1.234 ohms	L_7	0.0086 nH
R_8	0.573 ohms	L_8	0.0072 nH
C_1	1210.893 pF	C_5	170.681 pF
C_2	1459.601 pF	C_6	119.311 pF
C_3	1459.601 pF	C_7	173.755 pF
C_4	170.679 pF	C_8	98.0803 pF

3.5 Radiation Patterns

2D Radiation characteristics are calculated for both simulated and experimental analysis on 2.434, 3.76, and 4.564 GHz frequencies and compared in *Figure 8*. The proposed antenna design has optimal radiation characteristics in both planes E & H. Yet, tilt in radiation characteristics at upper band frequencies was observed; this could be due to the impact of a higher mode of operation at higher frequencies. Radiation patterns in 3D are also shown in *Figure 9*.

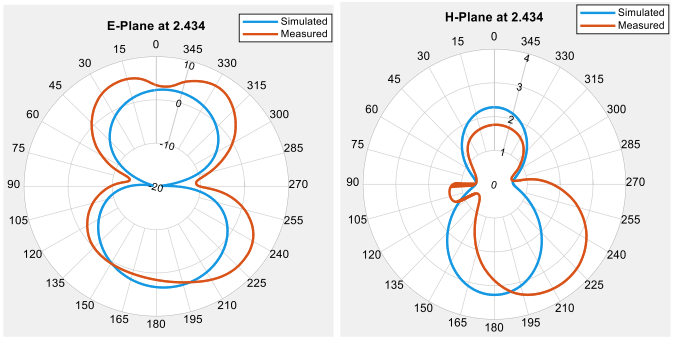

(a) *(b)*

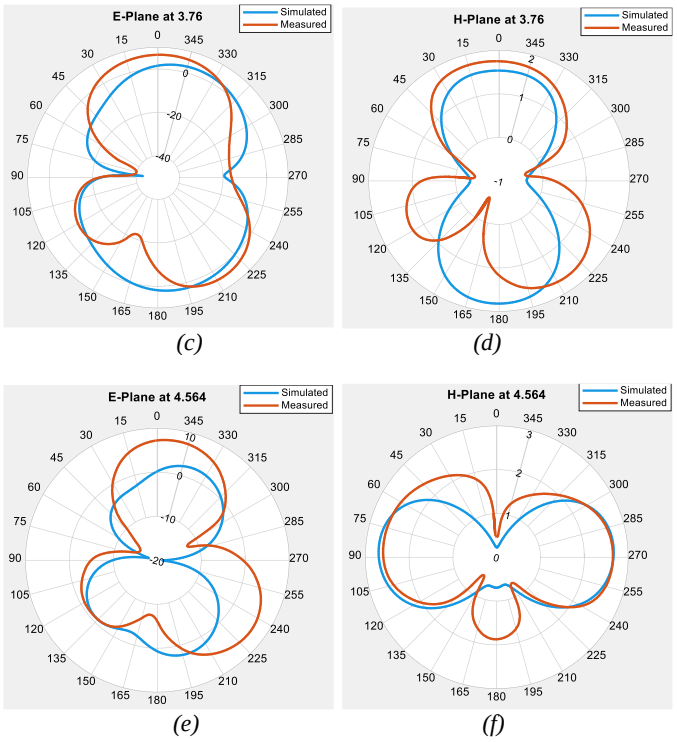

(c) *(d)*

(e) *(f)*

Figure 8: 2D Far-field Radiations Pattern at (a) E-Plane at 2.434GHz, (b) H-Plane at 2.434GHz, (c) E-Plane at 3.76 GHz, (d) H-plane at 3.76 GHz, (e) E-Plane at 4.564 GHz, (f) H-plane at 4.564 GHz

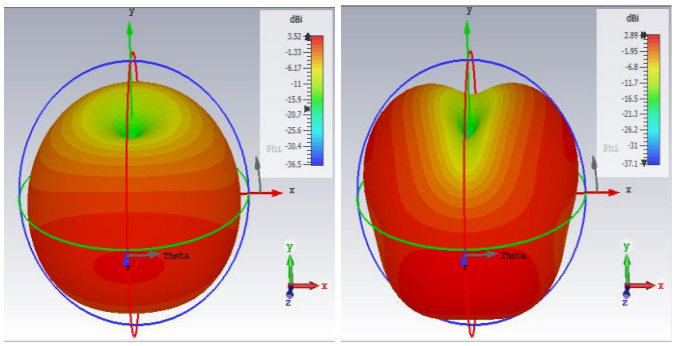

(a) 2.434GHz (b) 3.76 GHz

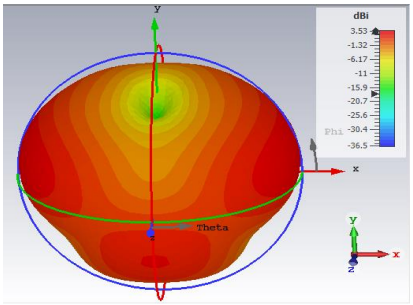

(c) 4.564 GHz

Figure 9: 3D Radiation Pattern on resonating frequencies

3.6 Surface Current Distribution

In the CST microwave simulator, the antenna has been tested on resonating frequencies for the surface current distribution.

FOREX Publication
Open Access | Rapid and quality publishing
International Journal of Electrical and Electronics Research (IJEER)
Research Article | Volume 9, Issue 4 | Pages 107-113 | e-ISSN: 2347-470X

For 2.434 GHz resonating frequency, it is visible that the current vectors are moving in two directions in the feedline just opposite of the notch made in the ground plane. The current vectors also move in the lower Ground towards the notch.

For 3.76 GHz frequency, current vectors are moving towards the top edge in the Patch. Some vectors move from the bottom triangle, some from the bottom of the feedline towards the middle of the feedline. Current vectors are moving towards the top in the ground plane and the feedline.

For 4.564 GHz, current in the triangle patch area travels towards the side edges center from the center of the triangle, top edges, bottom edges, and in the Ground, plane vectors are moving from top side corners towards lower bottom corners middle of the feet.

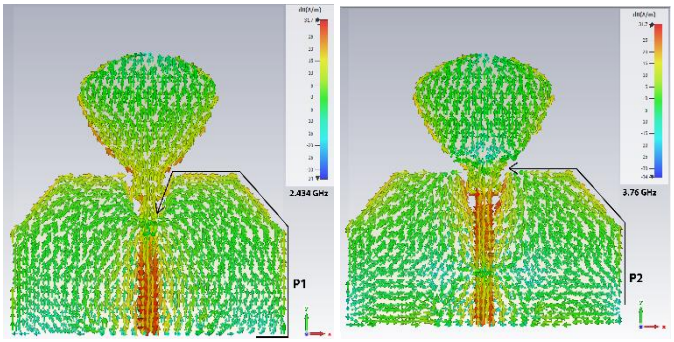

(a) 2.434GHz *(b) 3.76 GHz*

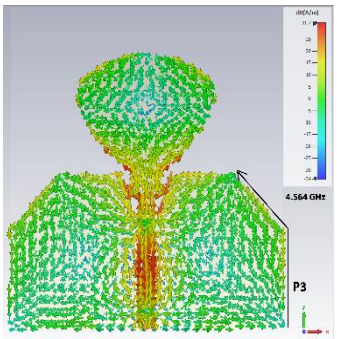

(c) 4.564 GHz

Figure 10: Surface Current Distribution of Proposed Antenna on Resonating Frequencies

3.7 VSWR, Gain and Efficiencies

The VSWR of the antenna is shown in *Figure 10*. The antenna's gain is shown in *Figure 11*; the highest gain achieved is 2.75 dBi on 4.564 GHz.

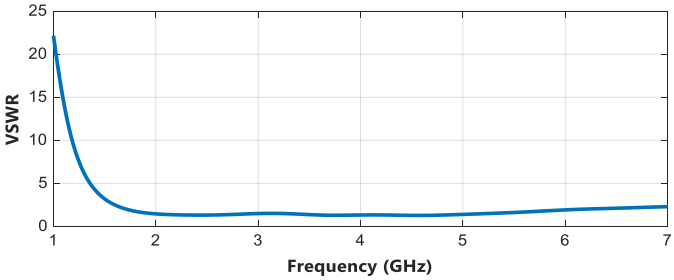

Figure 10: VSWR of Proposed Antenna

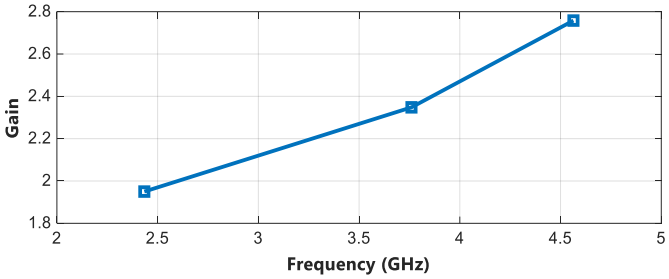

Figure 11: Gain of Proposed Antenna

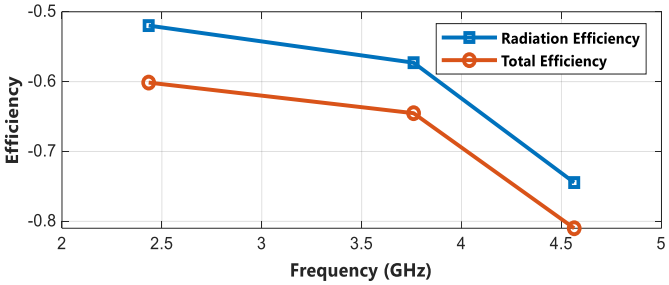

Figure 12: Efficiencies (Radiation and Total) of Proposed Antenna

Antenna efficiency is also shown in *Figure 12*. The radiation efficiencies are -0.5198, and total efficiency is -0.6014 at 2.434 GHz, -0.5729, and total efficiency is -0.6452 at 3.76 GHz, -0.7445, and total efficiency is -0.8099 at 4.564 GHz.

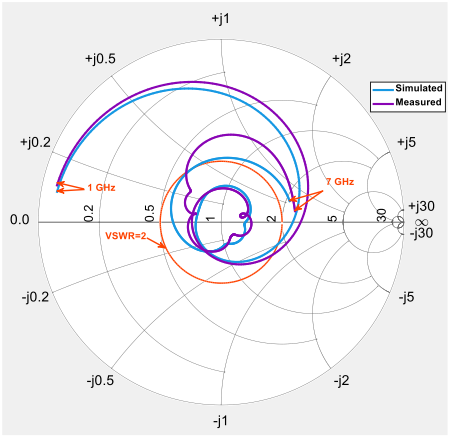

Figure 13: Impedance Chart

3.8 Antenna Impedance

Antenna impedance curves for simulated and measured outcomes are shown in *Figure 13*. It is observed that the multiple loops are found inside the VSWR circle indicates the mutual coupling and overlapping between resonating modes, which are essential for wide impedance bandwidth.

Table 5: Comparative study of proposed with antennas surveyed

References	f_l (GHz)	f_h (GHz)	BW (GHz)	Size(mm^2)
[8]	1.347	1.533	0.186	80×80
[9]	3.4	5.6	2.2	70×70
[10]	1.639	1.907	0.268	110×110
[11]	2.65	2.70	0.50	50×75
Proposed	1.7381	6.01	4.2719	60×65

FOREX Publication
Open Access | Rapid and quality publishing
International Journal of Electrical and Electronics Research (IJEER)
Research Article | Volume 9, Issue 4 | Pages 107-113 | e-ISSN: 2347-470X

The comparison of the surveyed antenna and proposed antenna is shown in *table 5*. From the table, it can be concluded that the proposed antenna has less size than other antennas and has larger bandwidth.

4. CONCLUSION

The experimented REULEAUX Triangle Shaped antenna instigating REULEAUX shaped Patch equipped with square-shaped element has been shown. The projected antenna demonstrates notable act with reflection coefficients < -10 dB in the wide operating band between 1.738 GHz and 6.01 GHz. The antenna found itself suitable for broadband wireless operations such as personal communication services (1.85-1.99 GHz), WiMAX (2.5 GHz, 3.5 GHz and 5.5 GHz) and WLAN (2.4 GHz, 5.2 GHz and 5.8 GHz). The antenna dimensions are adjusted using full-wave examination to attain ultra-wideband features, covering the 5G & WLAN applications. The antenna shows an impedance bandwidth of 4.272 GHz with the highest gain of 2.75 db. This explains that this antenna has an optimal radiation characteristic with such low-profile geometry, clearly visible in the antenna's radiation pattern. The performance characteristics such as antenna design, parametric analysis, input impedance, simulated surface current distribution, simulated and measured return loss, radiation pattern and gain of reported antenna has been found good to achieve wider operational band and ultra-wide band applications.

CONFLICTS OF INTEREST

The authors declare that there is no conflict of interest regarding the publication of this paper.

REFERENCES

[1] T. Ali, M. M. Khaleeq, S. Pathan, and R. C. Biradar, "A multiband antenna loaded with metamaterial and slots for GPS/WLAN/WiMAX applications," Microw. Opt. Technol. Lett., vol. 60, no. 1, pp. 79–85, Jan. 2018, doi: 10.1002/mop.30921.

[2] I. B. Vendik, A. Rusakov, K. Kanjanasit, J. Hong, and D. Filonov, "Ultrawideband (UWB) Planar Antenna with Single-, Dual-, and Triple-Band Notched Characteristic Based on Electric Ring Resonator," Antennas Wirel. Propag. Lett., vol. 16, pp. 1597–1600, 2017, doi: 10.1109/LAWP.2017.2652978.

[3] M. Yazdi and N. Komjani, "Planar UWB monopole antenna with dual band-notched characteristics for UWB applications," Microw. Opt. Technol. Lett., vol. 55, no. 2, pp. 241–245, Feb. 2013, doi: 10.1002/mop.27301.

[4] M. Moosazadeh and S. Kharkovsky, "A Compact High-Gain and Front-to-Back Ratio Elliptically Tapered Antipodal Vivaldi Antenna with Trapezoid-Shaped Dielectric Lens," Antennas Wirel. Propag. Lett., vol. 15, pp. 552–555, 2016, doi: 10.1109/LAWP.2015.2457919.

[5] L. J. Foged, A. Giacomini, and R. Morbidini, "Dual-Polarized Corrugated Horns for Advanced Measurement Applications," IEEE Antennas Propag. Mag., vol. 52, no. 6, pp. 199–204, Dec. 2010, doi: 10.1109/MAP.2010.5723270.

[6] P. H. Rao, S. Sujitha, and K. T. Selvan, "A Multiband, Mutipolarization Shared-Aperture Antenna: Design and evaluation.," IEEE Antennas Propag. Mag., vol. 59, no. 4, pp. 26–37, Aug. 2017, doi: 10.1109/MAP.2017.2706654.

[7] A. Chauloux, F. Colombel, M. Himdi, J.-L. Lasserre, and P. Pouliguen, "Low-Return-Loss Printed Log-Periodic Dipole Antenna," Antennas Wirel. Propag. Lett., vol. 13, pp. 503–506, 2014, doi: 10.1109/LAWP.2014.2310057.

[8] Kin-Lu Wong, Chien-Chin Huang, and Wen-Shan Chen, "Printed ring slot antenna for circular polarization," IEEE Trans. Antennas Propagat., vol. 50, no. 1, pp. 75–77, Jan. 2002, doi: 10.1109/8.992564.

[9] J.-Y. Jan and Jia, "Bandwidth enhancement of a printed wide-slot antenna with a rotated slot," IEEE Trans. Antennas Propagat., vol. 53, no. 6, pp. 2111–2114, Jun. 2005, doi: 10.1109/TAP.2005.848518.

[10] Jia-Yi Sze and Kin-Lu Wong, "Bandwidth enhancement of a microstrip-line-fed printed wide-slot antenna," IEEE Trans. Antennas Propagat., vol. 49, no. 7, pp. 1020–1024, Jul. 2001, doi: 10.1109/8.933480.

[11] R. P. S. Bhadoriya, "Directivity and Bandwidth Enhancement of Patch Antenna using Metamaterial," IJEER, vol. 9, no. 2, pp. 6–9, Jun. 2021, doi: 10.37391/IJEER.090201.

[12] R. A. Panda, M. Panda, P. K. Nayak, and D. Mishra, "Butterfly Shaped Patch Antenna for 5G Application," IJEER, vol. 8, no. 3, pp. 32–35, Sep. 2020, doi: 10.37391/IJEER.080301.

[13] M. Kate and A. Goen, "Comparison and Performance Evaluation on Microstrip Patch Antenna for WLAN Application," vol. 4, no. 3, p. 5, 2016.

[14] S. Dwivedi and S. S. Ojha, "Bandwidth Improvement of RMPA using DGS," IJEER, vol. 4, no. 1, pp. 30–32, Mar. 2016, doi: 10.37391/IJEER.040106.

[15] A. Narwaria and A. Duvey, "Simulation of Pentagon Shaped Multiband Antenna using Proximity Coupled Technique," IJEER, vol. 6, no. 2, pp. 45–47, Jun. 2018, doi: 10.37391/IJEER.060206.

[16] J.-Y. Jan and L.-C. Wang, "Printed Wideband Rhombus Slot Antenna With a Pair of Parasitic Strips for Multiband Applications," IEEE Trans. Antennas Propagat., vol. 57, no. 4, pp. 1267–1270, Apr. 2009, doi: 10.1109/TAP.2009.2015859.

[17] N. Sekeljic, Z. Yao, and H.-H. Hsu, "5G Broadband Antenna for sub-6 GHz Wireless Applications," in 2019 IEEE International Symposium on Antennas and Propagation and USNC-URSI Radio Science Meeting, Atlanta, GA, USA, Jul. 2019, pp. 147–148. doi: 10.1109/APUSNCURSINRSM.2019.8888509.

[18] G. Jin, C. Deng, J. Yang, Y. Xu, and S. Liao, "A New Differentially-Fed Frequency Reconfigurable Antenna for WLAN and Sub-6GHz 5G Applications," IEEE Access, vol. 7, pp. 56539–56546, 2019, doi: 10.1109/ACCESS.2019.2901760.

[19] T. Kiran, N. Mounisha, C. Mythily, and D. Akhil, "Design of Microstrip Patch Antenna for 5g Applications," IOSR Journal of Electronics and Communication Engineering, vol. 13, no. 1, pp. 14–17, Feb. 2018, doi: 10.9790/2834-1301011417.

[20] R. Azim, M. T. Islam, and N. Misran, "Microstrip Line-fed Printed Planar Monopole Antenna for UWB Applications," Arabian Journal for Science and Engineering, vol. 38, no. 9, pp. 2415–2422, Sep. 2013, doi: 10.1007/s13369-013-0553-x.